

UNCLASSIFIED

Defense Technical Information Center
Compilation Part Notice

ADP023741

TITLE: Organic Materials for Multiphoton Absorption: Time-Dependent
Density Functional Theory Calculations

DISTRIBUTION: Approved for public release, distribution unlimited

This paper is part of the following report:

TITLE: Proceedings of the HPCMP Users Group Conference 2007. High
Performance Computing Modernization Program: A Bridge to Future
Defense held 18-21 June 2007 in Pittsburgh, Pennsylvania

To order the complete compilation report, use: ADA488707

The component part is provided here to allow users access to individually authored sections
of proceedings, annals, symposia, etc. However, the component should be considered within
the context of the overall compilation report and not as a stand-alone technical report.

The following component part numbers comprise the compilation report:

ADP023728 thru ADP023803

UNCLASSIFIED

Organic Materials for Multiphoton Absorption: Time-Dependent Density Functional Theory Calculations

P.N. Day, K.A. Nguyen, and R. Pachter

US Air Force Research Laboratory, Materials & Manufacturing Directorate (AFRL/ML),
Wright-Patterson AFB, OH

{Paul.Day, Kiet.Nguyen, Ruth.Pachter}@wpafb.af.mil

Abstract

In our interest to accurately predict the photophysical properties of organic molecules that exhibit multiphoton absorption optical processes, we applied density functional theory (DFT)/time-dependent DFT (TDDFT) for the calculation of structures, and one-photon absorption (OPA), two-photon absorption (TPA) spectra, for series of relevant compounds. In our recent work TDDFT was validated regarding the exchange-correlation functional to be used for molecules that exhibit excited state charge-transfer characteristics, the application of quadratic response for TPA properties, and the inclusion of solvent effects, as applied, for example, to 4,4'-dimethyl-amino-nitrostilbene and a donor-acceptor (DA) fluorene-based system. In this work we discuss the prediction of TPA cross-section enhancements for large porphyrin dimers.

1. Introduction

Materials that exhibit TPA attracted significant interest in recent years due to applications in photodynamic therapy^[1,2], multiphoton microscopy^[3], photopolymerization^[4], and optical storage^[5]. At the same time, linear response TDDFT^[6] has become a useful and widespread tool in predicting OPA properties^[7]. Indeed, we have previously shown that by applying DFT^[8] and TDDFT with hybrid exchange-correlation (x-c) functional^[9], structures and OPA ground and excited spectra of porphyrins, and related material of interest for reverse saturable absorption could be accurately predicted. Effects of the chemical modification of Zn porphyrin were elucidated for meso-tetraaza substitutions and tetrabenzo annulations, explaining structural and spectral properties of these materials^[10]. A comparative study between TDDFT and TDHF for spectra of Zn porphyrin, Zn meso-tetraphenylporphyrin, and halogenated derivatives^[11], validated our calculations. For further

validation, we also examined a broad range of π -conjugated systems, in addition to free-base porphyrins, phthalocyanines, and their metal complexes^[12]. The average error for the calculated excitation energies was comparable to the results predicted by highly correlated ab initio methods, as was also demonstrated for quinoxaline porphyrin monomers^[13].

The prediction of TPA cross-sections is challenging^[14], and although the TPA cross-section can be calculated by invoking essential state models to the full sum-over-states approach, the required accuracy of the results motivated additional improvements. Recently we re-examined^[15] the calculated TPA spectra of 4,4'-dimethyl-amino-nitrostilbene^[16], as well as of AF-69, representing a large class of substituted fluorenes^[17].

In particular, we assessed improvements in comparison with experimental data by applying the Coulomb-attenuated method (CAM)-B3LYP (x-c) functional^[18], as well as a modified version (mCAM-B3LYP), to account for the change in charge-transfer characteristics. The importance of applying the appropriate (x-c) functional for charge-transfer has been recently further emphasized^[19]. In addition, the application of quadratic response within TDDFT was investigated^[20], proven important for the accuracy of the results, as well as the effects of solvent. Overall, we have shown that while the CAM-B3LYP (x-c) functional accurately predicted the excitation energies in DANS, our improved mCAM-B3LYP was more appropriate in predicting the excitation energies in AF-69, pointing out the importance of taking into account accurately the long-range exchange contribution. A good agreement was obtained for the TPA cross-sections, further validated for coumarins^[21], while the TPA characteristics of fluorene-based materials were also recently explained^[22,23].

In this work we report results for porphyrins (P), as recent studies^[24] showed a remarkable enhancement of the TPA cross-section in changing from a single porphyrin unit to porphyrin dimers linked by ethyne (y) or butadiyne (yy), e.g., for yPy as compared to PyP, emphasizing

however the challenge in comparing the predicted OPA and TPA with experimental values in this case. To carefully assess the (x-c) functional we carried out calculations also for porphyrin, in comparison with previous work, to be reported separately^[25].

2. Computational Details

In this study we follow the theoretical methods that we have previously outlined^[14,15]. The geometry of each system was optimized using B3LYP with a 6-31G** basis set^[26]. Linear response (LR), single residue quadratic response (SRQR), and double residue quadratic response (DRQR) TDDFT calculations were carried out with Dalton^[27]. Solvation effects were examined by applying the self-consistent reaction field model with a spherical cavity (SCRF-S), and also the polarizable continuum model (PCM). The solvent used in the OPA and TPA experimental spectra measurements for the zinc porphyrin systems was dichloromethane with 1% pyridine. In order to simulate the effect of the pyridine, the geometry of yPy was therefore re-optimized with one and two pyridine molecules coordinated to the zinc atom (see Figure 1). Results are reported for the system with one pyridine molecule, which will be denoted yPy(1pyr).

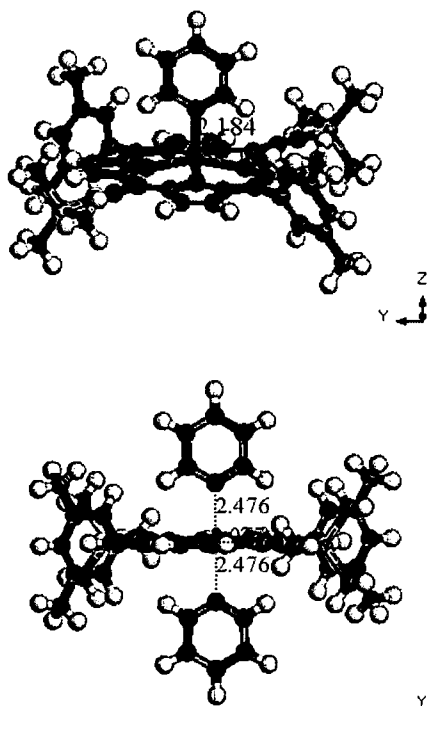


Figure 1. Structures of yPy(1pyr) and yPy(2pyr)

3. Results and Discussion

A. yPy

The addition of the ethynyl groups to the basic zinc porphyrin reduces the symmetry from D_{4h} to D_{2h} , red-shifts both the Q and B bands, and substantially strengthens the Q-band. While the Q-band is still weak compared to the B-band, the Gouterman four-orbitals are perturbed by this additional conjugation. The role of the intensity of the Q-band in TPA is evident from the three-state approximation for the centrosymmetric molecule, as the Q-band states are the primary intermediate state for the lowest TPA bands. Table 1 lists the calculated excitation energies and oscillator strengths for the Q and B states in comparison with experiment. The calculations using B3LYP were carried out with different basis sets and solvation models. Similar to porphyrin, the computed excitation energies and intensities are overestimated. Increasing the size of the basis set tends to red-shift the calculated Q and B states, resulting in better agreement with experiment, although adding diffuse functions seems to have little effect. The inclusion of a single pyridine molecule (p) coordinated to the zinc atom in yPy results in a more significant red-shift, particularly when using the PCM model, closer to the experimental data. However, the application of continuum solvation models increases the calculated intensity.

Table 1. Calculated Excitation Energies and Oscillator Strengths for yPy

		Q_y	Q_x	B_x	B_y	
B3LYP, no solvent; 6-31G**	ΔE	2.17	2.19	3.07	3.16	
	f	0.19	0.00	1.22	1.47	
B3LYP, no solvent; 6-311G**	ΔE	2.11	2.14	3.03	3.12	
	f	0.20	0.00	1.26	1.43	
B3LYP, no solvent; 6-311+G**	ΔE	2.15	2.16	3.03	3.10	
	f	0.18	0.00	1.12	1.43	
B3LYP, no solvent; 6-311++G**	ΔE	2.15	2.16	3.03	3.10	
	f	0.19	0.00	1.12	1.43	
B3LYP; 1p; 6-31G**	ΔE	2.09	2.14	2.99	3.11	
	f	0.21	0.00	0.99	1.14	
B3LYP; 1 p; 6-311G**	ΔE	2.06	2.12	2.96	3.05	3.08
	f	0.21	0.00	1.03	0.22	0.98
B3LYP; SCRF-S; 6-31G**	ΔE	2.18	2.20	3.07	3.14	
	f	0.23	0.00	1.25	1.67	
B3LYP; SCRF-S; 6-311G**	ΔE	2.16	2.18	3.04	3.10	
	f	0.23	0.00	1.26	1.63	

		Q_y	Q_x	B_x	B_y	
B3LYP; 1p+SCRF-S; 6-31G**	ΔE	2.08	2.14	2.97	3.07	3.10
	f	0.25	0.00	1.15	0.90	0.48
B3LYP; 1p+SCRF-S; 6-311G**	ΔE	2.05	2.12	2.94	3.04	
	f	0.25	0.00	1.16	1.28	
B3LYP; 1p+PCM; 6-31G**	ΔE	2.05	2.14	2.87	2.99	
	f	0.31	0.00	1.31	1.41	
B3LYP; 1p+PCM; 6-311G**	ΔE	2.03	2.12	2.85	2.97	
	f	0.31	0.00	1.34	1.41	
B3LYP; 1p+PCM; 6-311+G**	ΔE	2.01	2.10	2.80	2.93	
	f	0.31	0.00	1.31	1.37	
CAM-B3LYP; 1p; 6-31G**	ΔE	2.07	2.14	3.19	3.26	
	f	0.17	0.00	1.24	1.47	
CAM-B3LYP; 1p+PCM; 6-31G**	ΔE	2.04	2.13	3.06	3.13	
	f	0.26	0.00	1.52	1.69	
mCAM-B3LYP; 1p; 6-31G**	ΔE	2.10	2.16	3.06	3.19	3.13
	f	0.20	0.00	0.85	1.19	0.45
mCAM-B3LYP; 1p+PCM; 6-31G**	ΔE	2.07	2.16	2.95	3.05	
	f	0.30	0.00	1.41	1.55	
Measured; CH ₂ Cl ₂	ΔE	1.92	2.07	2.73	2.80	
	f	0.15	0.00	0.66	0.94	

The calculated absorption spectra applying different (χ -c) functionals, namely B3LYP, CAM-B3LYP, and mCAM, in comparison with experiment, with a pyridine coordinated to the porphyrin, are shown in Figure 2. The calculated CAM-B3LYP B-band is blue-shifted nearly 0.5 eV from experiment, compared to about 0.3 eV for B3LYP, with the mCAM value about midway between those two results. Upon applying PCM, this error is reduced to about 0.2 eV for B3LYP.

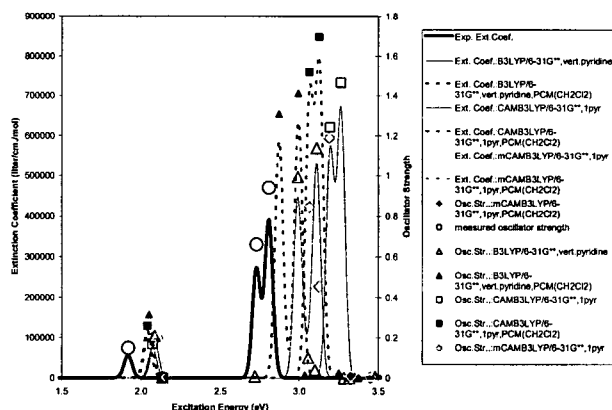


Figure 2. OPA spectra of yPy1pyr calculated using TDDFT with different functionals and 6-31G** basis set

The calculated Q-band excitation energy is closer to experiment and less dependent on the applied functional, as all three functionals predict this excitation energy to be less than 0.2 eV higher than measured, and in good agreement with the experimental intensity. When the PCM is included, the error is reduced to about 0.1 eV. The calculated and measured TPA spectra for yPy are reported elsewhere^[25]. It is shown that while the reported measured maximum TPA cross-section is about 20 GM at a transition energy of about 2.9 eV (corresponding to degenerate photons at 1.45 eV), the QRSR-TDDFT results predict a much larger cross-section at a higher transition energy. The over-prediction of the TPA cross-section can be attributed to the over-prediction of the energy of the two-photon state and resulting large resonance enhancement, as evident from Eq. (1), where the cross-section is estimated by the three-state approximation (type I)^[14]. In the case where the two incident photons have the same energy (E_λ), the cross-section δ is given by

$$\delta'_{f_0} = \frac{32\pi^4 g_{\max}}{15(ch)^2} \frac{E_\lambda^2}{(E_i - E_\lambda)^2} |\mu_{0i}|^2 |\mu_{if}|^2 (2 \cos^2 \Theta_{\mu\mu} + 1), \quad (1)$$

where g_{\max} is the maximum in the line width function, $\Theta_{\mu\mu}$ is the angle between the two transition dipole moment vectors. While the three-state approximation is often not adequate for quantitative results, it can be useful in analysing the origin of the TPA intensity. The transitions to the TPA states calculated to be near 3.6 eV require photons with an energy of 1.8 eV, which is close to resonant energy with the calculated one-photon states near 2.1 eV, in comparison with the measured TPA, which required photons near 1.5 eV. Applying CAM-B3LYP, a TPA was calculated near 4.28 eV, which is highly resonant with the OPA state calculated near 2.14 eV, thus resulting in an unphysically large result for the cross-section.

B. PyP

The OPA for PyP²⁵ shows that the calculated spectra tend to be blue-shifted and more intense than the experimentally measured data. However, the excitation energy calculated for the Q-band with the B3LYP functional is in excellent agreement with experiment. CAM-B3LYP results in Q-band blueshifts of 0.1 eV, and reduces the oscillator strength to 0.71.

The experimental B-band for PyP has a narrow intense peak at about 2.6 eV and a much broader feature peaking near 3.0 eV, with a combined oscillator strength of 2.91. The calculated B-bands are blue-shifted compared to experiment, and appear to be more intense than experiment. However, the combined CAM-B3LYP oscillator strength of the two states is in good agreement

with experiment, while B3LYP, which predicts two strong transitions and two weak transitions in this region, show a combined oscillator strength in good agreement with experiment.

The TPA for PyP is presented in Figure 3. Calculated results are given for both the bare PyP and with the two coordinated pyridines using both the B3LYP and CAM-B3LYP functionals. Experimentally, a strong TPA peak is observed, reaching 8,500 GM, near a transition energy of 3.0 eV. Applying B3LYP for the bare PyP, two smaller TPA features are predicted, one about 0.5 eV lower in energy than experiment and the other 0.5 eV higher than experiment. Including the two pyridines in the calculation induces a red-shift in the lower TPA peak, and while the position of the second peak does not change, the red-shift in the Q-band state brings it into resonance with this state causing an unphysically large result for this TPA cross-section. When CAM-B3LYP is used on the bare molecule, the first TPA peak is blue-shifted relative to experiment, but when the two pyridine molecules are included, excellent agreement with experiment is obtained. A peak TPA cross-section of about 15,000 GM is predicted near the transition energy of 3.06 eV, but the experiment did not go above 3.0 eV and the TPA cross-section is still increasing at that energy. This result highlights the challenge in accurate predictions, because the OPA calculated with CAM-B3LYP is not in as good an agreement with experiment.

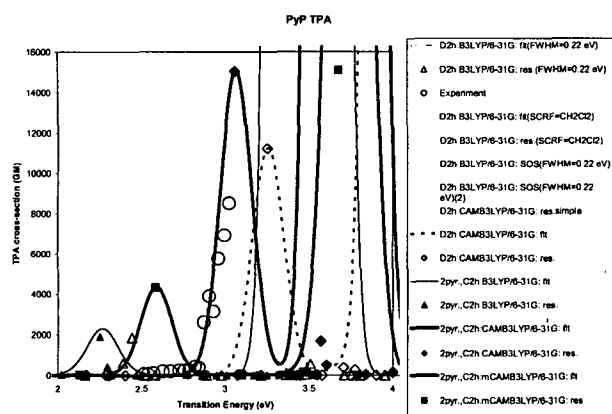


Figure 3. TPA spectra of PyP

4. Conclusions

In this work, we presented results of structures and spectra for porphyrin-based materials applying DFT/TDDFT, as potential systems to be examined for TPA applications, of significant interest. Although the accuracy of the results is mostly consistent with previous work, it is notable that challenges remain in theoretical and computational developments for attaining a predictive

capability for materials that exhibit nonlinear optical absorption.

Acknowledgments

This work has been supported by a DoD High Performance Computing Modernization Program Challenge Project WPAFMLW01543C21.

References

1. Arnbjerg, J., J.-B. Ana, M.J. Paterson, S. Nonell, J.I. Borrell, O. Christiansen, and P.R. Ogilby, *J. Am. Chem. Soc.*, 129, 5188, 2007.
2. Spangler, C.W., J.R. Starkey, F. Meng, A. Gong, M. Drobizhev, A. Rebane, and B. Moss, *Proceedings of SPIE-The International Society for Optical Engineering*, 5689, 141, 2005.
3. Williams, R.M., W.R. Zipfel, and W.W. Webb, *Curr. Opin. Chem. Biol.*, (2001) 5, 603.
4. Denny, L.R., J.W. Baur, M.D. Alexander, S.M. Kirkpatrick, and S.J. Clarson, *Polymer Preprints*, 41, 3, 2000.
5. Makarov, N., M. Drobizhev, A. Rebane, D. Peone, H. Wolleb, and H. Spahn, Heinz, *Proceedings of SPIE-The International Society for Optical Engineering*, 6330, 63300K/1, 2006.
6. Runge, E. and E.K.U. Gross, *Phys. Rev. Lett.*, 52, 997, 1984.
7. Dreuw, A. and M. Head-Gordon, *Chem. Rev.*, 105, 4009, 2005.
8. Wang, Z., P.N. Day, and R. Pachter, *Chem. Phys. Lett.*, 237, 45, 1995; Z. Wang, P.N. Day, and R. Pachter, *Chem. Phys. Lett.*, 248, 248, 1996; P.N. Day, Z. Wang, and R. Pachter, *J. Mol. Struct. Theochem*, 455, 33, 1998; V. Mastryukov, C-Y. Ruan, M. Fink, Z. Wang, and R. Pachter, *J. Mol. Struct.*, 556, 225, 2000.
9. Nguyen, K.A., P.N. Day, and R. Pachter, *J. Chem. Phys.*, 10, 9135, 1999; K.A. Nguyen, P.N. Day, and R. Pachter, *J. Phys. Chem.*, 103, 7378, 1999; K.A. Nguyen, P.N. Day, and R. Pachter, *J. Phys. Chem.*, 104, 4755, 2000.
10. Nguyen, K.A. and R. Pachter, *J. Chem. Phys.*, 114, 10757, 2001; K.A. Nguyen and R. Pachter, *J. Chem. Phys.*, 118, 5802, 2003.
11. Nguyen, K.A., R. Pachter, S. Tretiak, V. Chernyak, and S. Mukamel, *J. Phys. Chem.*, 106, 10285, 2002.
12. Nguyen, K.A., J. Kennel, and R. Pachter, *J. Chem. Phys.*, 117, 7128, 2002.
13. Smith, M.J., W. Clegg, K.A. Nguyen, J.E. Rogers, R. Pachter, P.A. Fleitz, and H.A. Anderson, *Chem. Comm.*, 2433, 2005.
14. Day, P.N., K.A. Nguyen, and R. Pachter, *J. Phys. Chem. B*, 109, 1803, 2005.
15. Day, P.N., K.A. Nguyen, and R. Pachter, *J. Chem. Phys.*, 125, 094103, 2006.
16. Antonov, L., K. Kamada, K. Ohta, and F. Kamounah, *Phys. Chem. Chem. Phys.*, 5, 1193, 2003.

17. Kannan, R., G.S. He, L. Yuan, F. Xu, P. N. Prasad, A.G. Dombroskie, B.A. Reinhardt, J.W. Baur, R.A. Vaia, and L.-S. Tan, *Chem. Mater.*, 13, 1896, 2001.
18. Yanai, T., D.P. Tew, and N.C. Handy, *Chem. Phys., Lett.*, 393, 51, 2004.
19. Magyar, R.J. and S. Tretiak, *J. Chem. Theory Comp.*, 3, 976, 2007.
20. Salek, P., O. Vahtras, T. Helgaker, and H. Agren, *J. Chem. Phys.*, 117, 9630, 2002.
21. Nguyen, K.A., P.N. Day, and R. Pachter, *J. Chem. Phys.*, 126, 094303, 2007.
22. Nguyen, K.A., J.E. Rogers, J.E. Slagle, P.N. Day, R. Kannan, L.-S. Tan, P. A. Fleitz, and R. Pachter, *J. Phys. Chem. A*, 110, 13172, 2006.
23. Nguyen, K.A., P.N. Day, and R. Pachter, *Theor. Chem. Acc.*, in press.
24. Drobizhev, M., Y. Stepanenko, Y. Dzenis, A. Karotki, A. Rebane, P.N. Taylor, and H.L. Anderson, *J. Am. Chem. Soc.*, 126, 15352, 2004; M. Drobizhev, Y. Stepanenko, Y. Dzenis, A. Karotki, A. Rebane, P.N. Taylor, and H.L. Anderson, *J. Phys. Chem. B*, 109, 7223, 2005.
25. Day, P.N., K.A. Nguyen, and R. Pachter, to be submitted.
26. Gaussian 03, <http://www.gaussian.com/>.
27. Dalton, <http://www.kjemi.uio.no/software/dalton/dalton.html>.